

# Estimation of ice thickness of the Satopanth Glacier, Central Himalaya using ground penetrating radar

Aditya Mishra<sup>1</sup>, B. D. S. Negi<sup>1</sup>, Argha Banerjee<sup>2</sup>, H. C. Nainwal<sup>1,\*</sup> and R. Shankar<sup>3</sup>

<sup>1</sup>Department of Geology, H.N.B. Garhwal University, Srinagar Garhwal 246 174, India

<sup>2</sup>Indian Institute of Science and Educational Research, Pune 411 008, India

<sup>3</sup>The Institute of Mathematical Sciences, Chennai 600 113, India

**Total volume of stored ice in the Himalayan glaciers is an important quantity for water resource management of the Himalayan catchments. However, direct measurement of glacier-ice thickness is rare in the Indian Himalaya. We have estimated the ice thickness of the debris-covered Satopanth Glacier (SPG) using a ground penetrating radar (GPR). Multiple bistatic, unshielded antennae with frequencies of 16, 20, 40 and 80 MHz were used for this purpose. We have done GPR surveys at various locations over the ablation zone of SPG. However, satisfactory results were obtained only on two transects. Near the glacier snout, a transverse GPR profile shows an ice thickness of  $38 \pm 3.5$ – $50 \pm 3.5$  m. We have obtained  $98 \pm 7$ – $112 \pm 7$  m ice thickness at a longitudinal transect in the upper ablation zone. To measure the speed of the radar waves in ice, a common midpoint survey was carried out. Our results for the speed of the electromagnetic waves are slightly lower than the standard values of such waves through pure ice.**

**Keywords:** Common midpoint survey, debris-covered glaciers, ground penetrating radar, ice thickness.

## Introduction

THE Himalayan cryosphere forms a huge reservoir of freshwater. However, the volume estimates of ice are currently uncertain, ranging from about 2300 to 6300 km<sup>3</sup> (refs 1, 2). This large uncertainty is partly due to the fact that ice thickness cannot be measured directly by remote-sensing techniques and is estimated using a variety of approximate models<sup>2–7</sup>. It is, therefore, important to perform direct field measurements of ice thickness for individual glaciers. Such data would help in better calibration and validation of the models, potentially leading to more accurate estimation of the volume of stored ice in the Himalaya. In this study, we estimate the ice thickness of

the Satopanth Glacier (SPG), Central Himalaya, using ground penetrating radar (GPR) survey.

GPR is a well-established technique to study subsurface features<sup>8,9</sup>. In the bistatic configuration that we have used for our surveys, pulses of radio waves are generated and transmitted by the transmitter antenna. The pulses propagate through the medium and generate reflections from subsurface inhomogeneities in the refractive index. These reflected signals are detected by the receiver antenna and are recorded as a function of time. The spatial pattern and depth of the subsurface features that cause the inhomogeneities can be reconstructed by an analysis of the measured delays in the reflected signals. In the context of a glacier, the reflectors could be englacial features like embedded boulders, crevasses, subglacial till, ice-flow features and the bedrock. The bedrock is distinguished from other englacial features by the fact that it is a spatially continuous reflector, unlike other localized objects. The resolution and penetration depth of GPR are determined by antenna frequency and electromagnetic properties of the surveyed materials<sup>9</sup>. Due to high rates of signal attenuation, penetration depths are greatly reduced in ice with high water content. The higher the electrical conductivity of the melt water, the stronger is the dissipation. Both these issues lead to serious difficulties in GPR studies of the Himalayan glaciers, more so for the debris-covered ones.

Ice-thickness measurements by GPR are sparse in the Himalaya. In the Indian Himalaya, possibly the first attempt to estimate thickness was made on Dokriani glacier of Central Himalaya using a 12.5 MHz central frequency antenna<sup>10</sup>. The ice thickness of this glacier calculated by GPR survey ranges from 15 to 25 m near the snout to 120 m in the accumulation zone. Ice-thickness measurements of this Patseo and Samudra Tapu glaciers in Chandra-Bhaga basin of Western Himalaya were made using 50, 100 and 500 MHz frequency antennae<sup>11</sup>. The depth of the Patseo Glacier at one location was estimated as 40 m, but ice thickness of the Samudra Tapu Glacier could not be measured using 50 and 100 MHz frequency antennae. GPR profile on a

\*For correspondence. (e-mail: nainwal61@gmail.com)

longitudinal transect of 400 m using a 16 MHz frequency antenna was used to estimate the thickness of Chhota Shigri Glacier in the Western Himalaya. The thickness was found to be 110–150 m for the surveyed area<sup>12</sup>. Another GPR survey was conducted on the Chhota Shigri Glacier using very low frequency (4.2 MHz) antenna<sup>13</sup>. Bedrocks were mapped in five transverse transects. The maximum depth for the transect in the region surveyed by Singh *et al.*<sup>12</sup> was reported to be 127 m. A similar GPR configuration was deployed on Mera Glacier in Nepal Himalaya to estimate ice thickness<sup>14</sup>. Two cross-sections were successfully obtained showing maximum ice thickness more than 100 m. GPR survey was conducted on Yala Glacier, Langtal Himalaya, Nepal with 270 MHz frequency antenna to estimate ice thickness and the results showed mean thickness of 36 m with maximum 61 m (ref. 15). For all the glaciers mentioned above, successful ice-thickness measurements were done in debris-free regions. GPR studies in glaciers with extensive debris cover pose extra difficulties due to scattering and attenuation of the signals. To our knowledge, no successful attempt has been reported so far in the Indian Himalaya, for thickly debris-covered glaciers. However, GPR studies have been reported from debris-covered Lirung and Khumbu glaciers in Nepal<sup>16</sup>.

GPR directly measures the two-way travel time (TWT), the time taken for the pulse to propagate from the transmitter to the reflector and back to the receiver. Estimation of the depth of the reflector from these data requires the speed of the radio wave in the medium as input. The speed of the radio waves through bubble-free pure ice is well established to be 0.167 m/ns (refs 17 and 18). However, the presence of impurities could change this value. In glaciers with extensive supra-glacial debris, we expect to have englacial debris as well. So, it is important to measure the speed of the radio waves in the glacier being studied.

In this article, we report on ice-thickness measurements made on SPG using a GPR survey. We have obtained reflections showing subsurface features, including the bedrock, at two transects on the SPG. We have also performed the common midpoint (CMP) analysis to measure the speed of radar-wave propagation in the study area. To best of our knowledge, there have been no CMP surveys reported earlier for any Indian Himalayan glacier. We discuss the effects of varying the frequency and configuration of the antennae.

## Study area

SPG is a compound valley glacier located in the Alaknanda Valley, Central Himalaya, Chamoli district, Uttarakhand, India (Figure 1). It is an easterly-flowing glacier, covering a length of about 13 km with average width of the main trunk being about 750 m. The average surface slope of the glacier is 5.4°, and the elevation

ranges from 3870 to 5800 m amsl. The equilibrium line altitude (ELA) is estimated to be about 5000 m (ref. 19). The glacier has extensive debris cover in the ablation zone. SPG is the source of the Alaknanda, a major tributary of River Ganga. Geologically, the study area lies north of the Main Central Thrust in the Higher Himalayan Crystalline Zone that has granitic gneisses, kyanite–sillimanite–garnet schist, and pegmatitic and aplitic veins as predominant lithological units belonging to Pindari Formation of Vaikrita Group<sup>20</sup>. Chronological study of glaciated landforms present in the upper Alaknanda valley is suggestive of various stages of glaciation in the valley. Among the stages that were identified by Nainwal *et al.*<sup>21</sup>, the oldest is known as Alaknanda stage that predates Last Glacial Maximum (LGM) followed by Alkapuri stage (12 ka) and Satopanth stage (4.5 ka)<sup>21</sup>. Recent studies show that the SPG terminus has retreated at a rate of  $5.7 \pm 0.6 \text{ m a}^{-1}$  from 1936 to 2013, with a measured area loss of  $0.27 \pm 0.05 \text{ sq. km}$  from 1956 to 2013. A study also revealed an average thinning of glacial ice in the lower ablation zone of SPG by  $9 \pm 11 \text{ m}$  in the past 51 years<sup>22</sup>.

## Methodology

A Geophysical Survey System Inc. (GSSI)-make GPR with subsurface interface radar (SIR) – 4000 control unit and multiple low frequency, bistatic, unshielded antennae were used in the study. The surveys were carried out in May and September 2016, in several locations in the ablation zone of the SPG. A total of 25 GPR transects of variable lengths were recorded between the snout and ELA using 16 and 20 MHz frequency antenna. Twenty profiles out of these 25 were below an elevation of 4300 m amsl and are in the thickly debris-covered region.

## GPR survey

In all the measurements, GPR survey was carried in point-measuring mode in which the transmitter (Tx) and

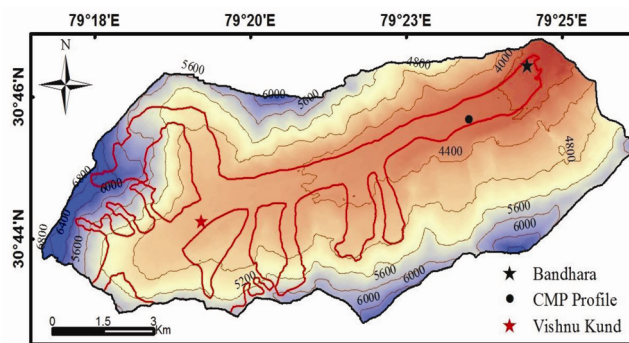


**Figure 1.** Map of Satopanth Glacier showing locations of GPR profiles. Red line indicates the glacier boundary while black line shows the basin boundary.

receiver (Rx) were shifted together in steps of 1 m, throughout maintaining a constant separation between them. The separation between Tx and Rx was fixed to be half of the wavelength of the radar wave in medium. Table 1 provides details of the other input parameters of the GPR system such as signal-transmit rate, samples/scans, etc. that were used in the study. These parameters were set by following the recommendations given in the GSSI manual. However, we have slightly modified the values in some cases to obtain satisfactory radargrams. The survey procedure adopted was as follows: a signal was triggered through control unit and confirmed through a trace in the display unit. Tx and Rx were then shifted forward with fixed separation between them and the same process was repeated throughout the survey. The surface positions and elevations of GPR survey line were measured using a Trimble R6 differential global positioning system (DGPS) which has an accuracy of about 1 cm in the point-to-point kinematic (PPK) mode. The data were processed using the software supplied by the manufacturer.

The standard routine was followed to process the GPR data using the RADAN 7 software of GSSI. The 'position correction' or 'time zero' was applied to the raw data. This was followed by background removal and filtering of the data using two types of filters – finite-impulse response (FIR) and infinite-impulse response (IIR). The values of high-pass and low-pass filters were fixed depending upon the antenna frequency. Deconvolution that removes multiple reflections between subsurface objects and antenna was then applied to the data. Finally, the gains at different TWT ranges were adjusted appropriately.

There are many reflections from englacial features in the processed radargrams. For any localized reflector, as it is approached, the distance from the reflector to the antennae decreases, reaches a minimum and then increases. Thus, the TWT also follows this pattern and can be seen as hyperbolas in the trace in the radargrams (Figure 2). While there could be steps and other sharp features, the distance from the antennae and bedrock, normally changes very slowly, leading to a continuous and slowly

changing TWT. Thus, in Figures 4 and 5, we have identified the bedrock with the first continuous reflection. We have also checked for consistency with other expected features of the bedrock. First, we expect the reflections from the bedrock to be stronger than those from englacial features. Secondly, as we move in the transverse direction away from the centre, we expect the depth to decrease.

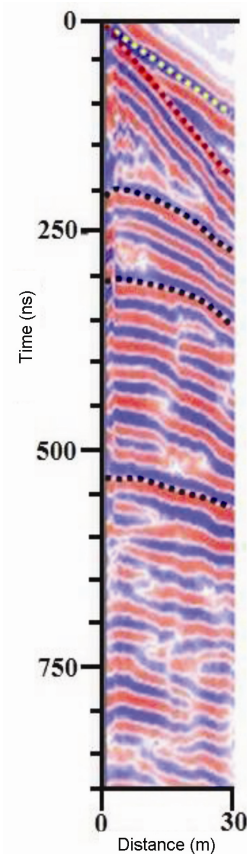


**Figure 2.** The common midpoint radargram. Yellow dots are the direct air waves, red dots the direct ground waves and black dots are waves reflected from englacial reflectors.

**Table 1.** Details of input and data acquisition parameters used during the ground penetrating radar survey

Input parameters	Bandhara profile	Vishnu Kund profile
Frequency (MHz)	20	16
Antenna separation (m)	4.8	6
Step count (m)	1	1
Signal transmit rate (kHz)	25	25
Samples/scan	2048	2048
Depth range (m)	100	300
Gain points	5	7
Static stacking	32	32
High pass filter (FIR)	10	5
Low pass filter (FIR)	30	40

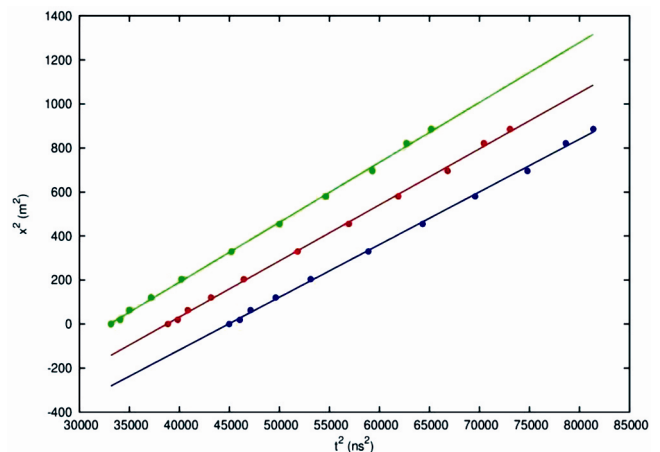


**Figure 3.** Common midpoint plot.

Finally, as we move in the upstream direction, we expect the depth to increase since we are in the ablation zone. The estimated depths were then calculated from the TWT and the speed of the radio waves measured by the CMP survey. The bedrock elevations were calculated by subtracting the measured depths from the surface elevations measured by the DGPS survey.

**CMP survey**

The speed of the radio waves in the medium is a crucial input parameter for GPR studies. As mentioned earlier,

this may depend on the ice composition and structure. Hence it can vary slightly from glacier to glacier. So, to get accurate depth estimations, it is necessary to accurately measure the radio-wave speed in the glacier being studied. We have used the CMP method to measure the speed of radio waves in the study region. Figure 1 shows the location of the CMP survey. The debris thickness in the region is about 30 cm. The survey was done using a 20 MHz antenna. In the survey, Tx and Rx were initially placed together and a trace was taken. Then both were moved away from each other, increasing in steps of 2 m till a separation of 30 m. Using this procedure, three types of signals were recorded – those due to the direct air waves, direct ground waves and waves reflected from

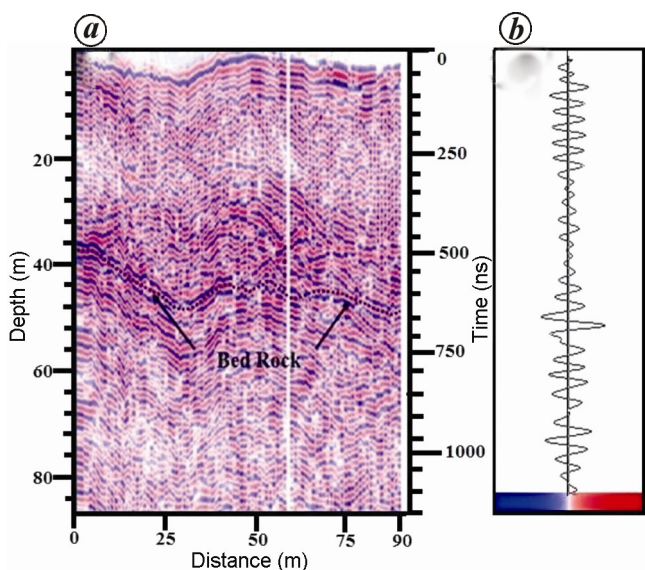


**Figure 4.** (a) GPR profile of Satopanth Glacier along a transverse transect at Bandhara (near the snout) and (b) its average corresponding trace window (or oscilloscope) showing amplitude of reflected waves in the surveyed medium.

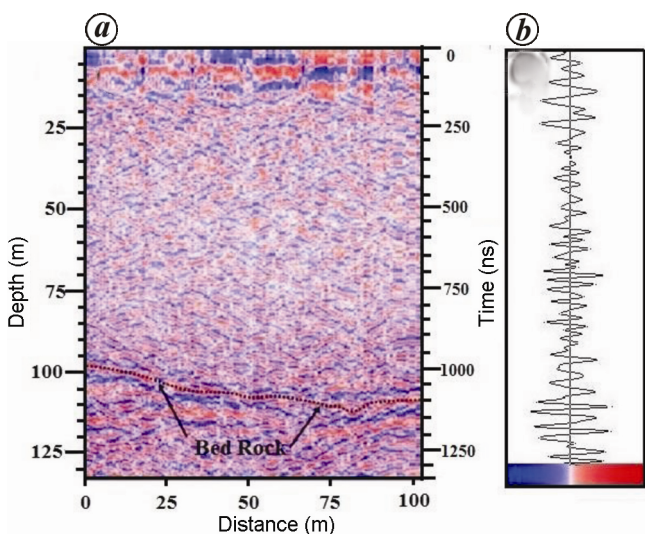


**Figure 5.** (a) GPR profile of Satopanth Glacier along a longitudinal transect at Vishnu Kund (~9 km upstream from the snout) and (b) its average corresponding trace window (or oscilloscope) showing amplitude of the reflected waves in the surveyed medium.

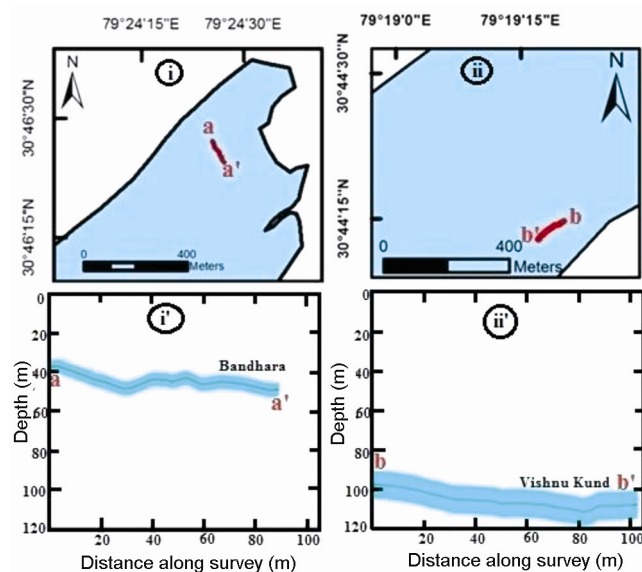


**Figure 6.** Results of GPR profiles with location. Positions of (i) Bandhara (transverse) and (ii) Vishnu Kund (longitudinal) profiles and their corresponding measured depths (i' and ii') are shown. The blue band indicates uncertainties in the estimations.

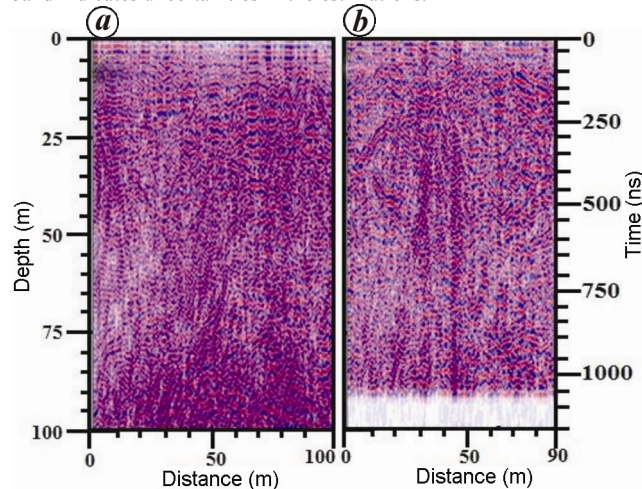


**Figure 7 a and b.** Radargrams with 20 MHz between Bandhara and Vishnu Kund. At this frequency no bedrock reflections could be observed.

the subsurface features. The travel time for the direct waves varies linearly with the separation and is seen as straight lines (yellow and red dotted lines) in Figure 2. The speed of the radio waves through air and ground can be obtained from the slopes of these straight lines. Assuming a homogeneous medium, the TWT for the reflected wave has a hyperbolic profile given by the equation<sup>8</sup>

$$(ct)^2 - x^2 = (2z)^2, \quad (1)$$

where  $c$  is the speed of the radio waves,  $t$  the TWT,  $x$  the separation between the antennae, and  $z$  is the depth of the reflector.

We plot the measured  $x^2$  against  $t^2$  and fit a straight line. The speed of the wave and depth of the reflector are obtained as the square roots of the slope and intercept of this best-fit straight line. This value of  $c$  is used to convert TWT into depth values.

### Uncertainty analysis

All our estimates are based on TWT. The radargram shows red and blue bands (Figure 2). These are the false colours indicating the positive and negative values of the electric field of the reflected waves. We have measured  $t$  using the points between the red and blue bands in the traces shown in Figure 2. However, the reflection could have taken place anywhere between the top of the blue band to the bottom of the red band. The width of the bands, namely the time interval from the top of the blue band to the bottom of the red band is about 15 ns. Therefore, we take 15 ns to be the uncertainty in the TWT, i.e. the actual TWT can be anywhere between  $t + 15$  ns and  $t - 15$  ns.

Next, we discuss the uncertainty in the speed measured by the CMP method. As discussed in the previous section we get the speed and reflector depth as the slope and intercept of the straight line obtained by plotting the measured values of  $x^2$  against  $t^2$ . We denote values thus obtained by  $c$  and  $z$ . However, the actual TWT can be anywhere between  $t + 15$  ns and  $t - 15$  ns. Consequently, there is a range of possible values of  $c$  and  $z$ . To determine this range, we plot  $x^2$  against  $(t \pm 15 \text{ ns})^2$  to get  $c \pm \Delta c$  and  $z \pm \Delta z$ .

## Results

### Wave speed

Three clear reflections were manually traced out from the CMP data (Figure 2). The procedure detailed in the previous section was applied to them. Figure 3 shows the straight lines obtained by plotting  $x^2$  against  $(t - 15 \text{ ns})^2$  (green),  $t^2$  (red) and  $(t + 15 \text{ ns})^2$  (blue). Table 2 shows the wave speeds and reflector depths obtained from the anal-

ysis. While the speeds obtained from the first two reflections differ by 0.004 m/s, whereas uncertainties are 0.005 m/s. They are hence the same up to the uncertainties. The speed obtained from the third is a little lower. More data are required to deduce if this is part of a systematic trend or due to some unknown error. Therefore, in this work we take the speed to be the average, i.e.  $c = 0.156 \pm 0.008$  m/ns; the error estimate being the standard deviation. This is about 7% smaller than the pure ice value of 0.167 m/ns (refs 17 and 18). This is the radio-wave speed that we have used for depth estimation.

### Bedrock reflections

We could clearly identify possible bedrock reflections at only two locations – one in the vicinity of the terminus of the glacier, which we refer to as Bandhara and another about 9 km upstream of the terminus, which we refer to as Vishnu Kund (Figure 1). Bandhara has thick (about 1 m) supra-glacial debris cover whereas in Vishnu Kund, the supra-glacial debris is very thin, only a few centimetres. In Figure 4, the continuous reflections are traced out for Bandhara. As can be seen, there are several reflections above the identified bedrock. However, none of these is truly continuous; they all have a hyperbolic shape which is characteristic of localized reflectors and they are also significantly weaker than the reflections corresponding to the identified bedrock. Therefore, we have attributed them to localized englacial features and not to the bedrock. The localized reflections are present in the Vishnu Kund radargram as well (Figure 5), but they are much weaker and the bedrock identification is clearer.

The uncertainty in the wave speed ( $0.156 \pm 0.008$  m/s) is about 2%. The uncertainty in the TWT is about 15 ns in about 500 ns, i.e. about 3%. Considering the fact that these uncertainties may be underestimated, we assume both to be 5%. The depths are estimated by  $d = c \times t/2$ . We estimate uncertainty in the depth using the standard formula

$$(\Delta d/d)^2 = (\Delta c/c)^2 + (\Delta t/t)^2. \quad (2)$$

This gives an uncertainty of about 7% in our depth estimations. Figure 6 shows the estimated ice thickness in the two locations, i.e. Bandhara and Vishnu Kund along with the corresponding uncertainties with respect to their positions.

**Table 2.** Speed of radio waves and reflector depths extracted from common midpoint analysis

Reflection	Wave speed (m/ns)	Reflector depth (m)
1	$0.160 \pm 0.005$	$15.7 \pm 0.75$
2	$0.164 \pm 0.005$	$25.0 \pm 1.5$
3	$0.145 \pm 0.002$	$38.50 \pm 0.5$

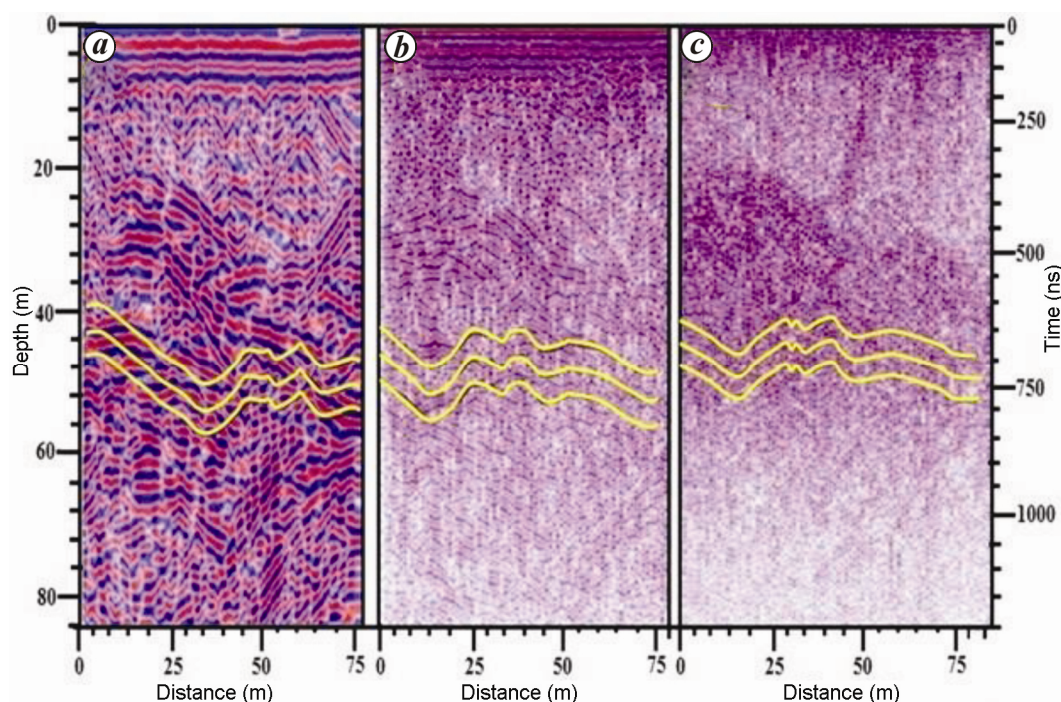


**Figure 8.** Radargrams at frequencies 16 (a), 40 (b) and 80 MHz (c), near Bandhara profile depicting consistency with the profile of 20 MHz (Figure 4). The depths with uncertainty ranges of the Bandhara profile of 20 MHz are plotted (yellow solid lines) over these radargrams.

## Discussion

A prominent feature of our GPR scans is the presence of a large number of englacial reflectors. SPG is a strongly avalanche-fed glacier<sup>19</sup>. Hence, we may expect a lot of debris to be deposited in the accumulation zone. This debris would submerge into the ice leading to a large number of englacial reflectors. The presence of a large number of englacial reflectors weakens the signal due to scattering, which makes the detection of the bedrock difficult. In the region between Bandhara and Vishnu Kund, we have surveyed several profiles as stated above. In each of these surveys a large number of englacial reflectors were seen; however, it was not possible to make out the continuous signal of the bedrock from these radargrams. Figure 7 shows two examples of such radargrams.

The following three factors may be relevant for this. First, in temperate glaciers, the water content is high compared to cold glaciers. Consequently, the radio wave dissipation is more. Secondly, in the regions of thick supra-glacial debris, the surface is extremely uneven and therefore the coupling between the antenna and the ground could be poor. Thirdly, in debris-covered glaciers there is a lot of englacial debris. This causes many reflections which weaken the signal due to scattering and could also mask the bedrock reflections.

We may have got good bedrock reflections in Bandhara, despite thick supra-glacial debris cover and many englacial features, because the ice thickness is small and con-

sequently the bedrock reflections are strong enough and not masked by the noisy englacial reflections. In Vishnu Kund, another transect where the bedrock could be mapped, ice thickness was large but the supra-glacial debris was thin and there were less reflections from englacial features.

GPR survey was carried at Bandhara with multiple frequencies (16, 40 and 80 MHz) to check their applicability at the location as well as for validation of the profile of 20 MHz at the same location. In Figure 8, the depths with uncertainty ranges of Bandhara profile of 20 MHz are plotted (yellow solid lines) over these radargrams. All these profiles are consistent with the 20 MHz frequency antenna; however, reflections are not as clear in the 20 MHz profile.

During acquisition of these profiles, different step sizes, i.e. the distance between two consecutive point measurements, were used. It was found that a step size of about 1 m or less gave good results.

## Conclusion

We have carried out GPR surveys at 25 transects in the ablation zone of the SPG, a debris-covered glacier in Central Himalaya. We could identify clear bedrock reflections in only two cases.

This low success rate illustrates that there are several difficulties in depth estimation by GPR in glaciers with a

thick supra-glacial debris cover. First, in temperate glaciers, the moisture present dampens the signal. Secondly, the thick supra-glacial debris cover makes the poor coupling between the antenna and the ground. Thirdly, there is a lot of noise from the englacial debris.

We performed a CMP survey to measure radio wave speed in the SPG. This was found to be  $0.156 \pm 0.008$  m/ns, which differs from the pure ice value of  $0.167$  m/ns by about 7%.

We have used this value of speed to estimate ice thickness of the SPG at two locations. Thickness near the snout, i.e. Bandhara was found to be  $37.5 (\pm 3.5)$  m at one end with maximum  $49.50 (\pm 3.5)$  m for this 90 m profile. At Vishnu Kund, located 9 km upstream to the snout in the upper ablation zone where supraglacial debris is a few centimetres thick, glacier ice thickness varied from 98 to  $112(\pm 7)$  m.

1. Bolch, T. *et al.*, The state and fate of Himalayan glaciers. *Science*, 2012, **336**, 310–314.
2. Frey, H. *et al.*, Estimating the volume of glaciers in the Himalayan–Karakoram region using different methods. *Cryosphere*, 2014, **8**, 2313–2333.
3. Oerlemans, J. *et al.*, Modelling the response of glaciers to climate warming. *Climate Dyn.*, 1998, **14**, 267–274.
4. Farinotti, D., Huss, M., Bauder, A. and Funk, M. and Truffer, M., A method to estimate ice volume and ice thickness distribution of Alpine glaciers. *J. Glaciol.*, 2009, **55**(191), 422–430.
5. Huss, M. and Farinotti, D., Distributed ice thickness and volume of all glaciers around the globe. *J. Geophys. Res.*, 2012, **117**(F4), F04010.
6. Gantayat, P., Kulkarni, A. V. and Srinivasan, J., Estimation of ice thickness using surface velocities and slope: case study at Gangotri Glacier, India. *J. Glaciol.*, 2014, **60**(220), 277–282.
7. Bahr, D. B., Meier, M. F. and Peckham, S. D., The physical basis of glacier volume–area scaling. *J. Geophys. Res.*, 1997, **102**(B9), 20355–20362.
8. Annan, A. P., GPR – History, trends, and future developments. *Subsurf. Sensing Technol. Appl.*, 2002, **3**(4), 253–270.
9. Jol, H. M., *Ground Penetrating Radar: Theory and Applications*, Elsevier, Great Britain, 2009.
10. Gergan, J. T., Dobhal, D. P. and Kaushik, R., Ground penetrating radar ice thickness measurements of Dokriani bamak (glacier), Garhwal Himalaya. *Curr. Sci.*, 1999, **77**, 169–173.
11. Singh, K. K., Kulkarni, A. V. and Mishra, V. D., Estimation of glacier depth and moraine cover study using ground penetrating radar (GPR) in the Himalayan region. *J. Indian Soc. Remote Sensing*, 2010, **38**, 1–9.
12. Singh, S. K., Rathore, B. P., Bahuguna, I. M., Ramanathan, A. L. and Ajai, Estimation of glacier ice thickness using ground penetrating radar in the Himalayan region. *Curr. Sci.*, 2012, **103**(1), 68–73.
13. Azam, M. F. *et al.*, From balance to imbalance: a shift in the dynamic behaviour of Chhota Shigri glacier, western Himalaya, India. *J. Glaciol.*, 2012, **58**, 315–324.
14. Wagnon, P. *et al.*, Seasonal and annual mass balances of Mera and Pokalde glaciers (Nepal Himalaya) since 2007. *Cryosphere*, 2013, **7**, 1769–1786.
15. Sugiyama, S., Fukui, K., Fujita, K., Tone, K. and Yamaguchi, S., Changes in ice thickness and flow velocity of Yala Glacier, Langtang Himal, Nepal, from 1982 to 2009. *Ann. Glaciol.*, 2013, **54**(64), 157–162.
16. Gades, A., Conway, H., Nereson, N., Naito, N. and Kadota, T., Radio echo-sounding through supraglacial debris on Lirung and Khumbu Glaciers, Nepal Himalayas. In *Debris-Covered Glaciers* (eds Nakawo, M., Raymond, C. F. and Fountain, A.), IAHS. Washington, USA, 2000, pp. 13–24.
17. Robin, G. Q., Velocity of radio waves in ice by means of a bore-hole interferometric technique. *J. Glaciol.*, 1975, **15**(73), 151–159.
18. Hubbard, B. and Glasser, N., *Field Techniques in Glaciology and Glacial Geomorphology*, Wiley and Sons Ltd, Chichester, England, 2005.
19. Laha, S. *et al.*, Evaluating the contribution of avalanching to the mass balance of Himalayan glaciers. *Ann. Glaciol.*, 2007, 1–9; doi:10.1017/aog.2017.27.
20. Valdiya, K. S. and Goel, O. P., Lithological subdivision and petrology of the Great Himalayan Vaikrita Group in Kumaun, India. *Proc. Indian Acad. Sci.*, 1983, **92**(2), 141–163.
21. Nainwal, H. C., Chaudhary, M., Rana, N., Negi, B. D. S., Negi, R. S., Juyal, N. and Shinghvi, A. K., Chronology of the Late Quaternary glaciation around Badrinath (Upper Alaknanda Basin): Preliminary observations. *Curr. Sci.*, 2007, **93**(1), 90–96.
22. Nainwal, H. C., Banerjee, A., Shankar, R., Semwal, P. and Sharma, T., Shrinkage of Satopanth and Bhagirath Kharak Glaciers 2 from 1936 to 2013. *Ann. Glaciol.*, 2016, **57**(71), 131–139.

ACKNOWLEDGEMENTS. We thank the Science and Engineering Research Board, Department of Science and Technology (DST), New Delhi for financial support under the special Himalayan Glaciology Programme (DST Grant No. SB/DGH-101/2015). A.M. thanks Mr Prabhat Semwal for assistance. We also thank our field assistants Mr Surendra Singh Badwal and Mr Gajendra Singh Badwal for help in the tough Himalayan glacier field during the study.

doi: 10.18520/cs/v114/i04/785-791